Journal of Applied Remote Sensing

RemoteSensing.SPIEDigitalLibrary.org

Assessing the calibration differences in the reflective solar bands of Terra MODIS and Landsat-7 enhanced thematic mapper plus

Amit Angal
Xiaoxiong Xiong
Dennis Helder
Morakot Kaewmanee
Larry Leigh

SPIE.

Amit Angal, Xiaoxiong Xiong, Dennis Helder, Morakot Kaewmanee, Larry Leigh, "Assessing the calibration differences in the reflective solar bands of Terra MODIS and Landsat-7 enhanced thematic mapper plus," *J. Appl. Remote Sens.* **12**(4), 044002 (2018), doi: 10.1117/1.JRS.12.044002.

Assessing the calibration differences in the reflective solar bands of Terra MODIS and Landsat-7 enhanced thematic mapper plus

Amit Angal,[a,*] Xiaoxiong Xiong,[b] Dennis Helder,[c] Morakot Kaewmanee,[c] and Larry Leigh[c]

[a]Science Systems and Applications Inc., Lanham, Maryland, United States
[b]NASA GSFC, Sciences and Exploration Directorate, Greenbelt, Maryland, United States
[c]South Dakota State University, Image Processing Lab, Brookings, South Dakota, United States

Abstract. Long-term data records obtained from Earth observing sensors depend not only on the calibration accuracy of individual sensors but also on the consistency across instruments and platforms. Hence, sensor calibration intercomparison plays a vital role for a better understanding of various science products. The Moderate Resolution Imaging Spectroradiometer (MODIS) and enhanced thematic mapper plus (ETM+) on the Terra and Landsat 7 platforms have operated successfully since their launch, collecting measurements in the reflective solar and infrared parts of the spectrum. Terra MODIS has employed a reflectance-based calibration since beginning its mission. In the case of ETM+, a radiance-based calibration was employed until recent years, when a reflectance-based calibration was introduced. Being in the AM constellation with less than 30 min difference in overpass times, near-simultaneous Earth scene measurements can be effectively used to assess the calibration differences between the spectrally matching bands of these two instruments. The pseudoinvariant calibration sites (PICS) in the North African desert are widely used for on-orbit calibration and validation of satellite sensors. Four PICS from this region have been employed to assess the multitemporal reflectance differences. Correction for bidirectional reflectance, spectral response function mismatch, and impacts of atmospheric water-vapor have been incorporated to provide an assessment of the long-term stability of each spectral band and reflectance differences amongst them. Results indicate that the spectral bands of both instruments show a long-term stability to within 2% from 2000 to 2017. The top-of-atmosphere reflectances between the two instruments postcorrection agree to within 4%. Also included in this paper is a detailed discussion of various parameters contributing to the uncertainties of this cross-calibration. The techniques presented in this paper can be further extended to perform similar intercomparison between Landsat 8 Operational Land Imager, Aqua MODIS, and Suomi-NPP VIIRS. [DOI: 10.1117/1.JRS.12.044002]

Keywords: Moderate Resolution Imaging Spectroradiometer; Terra; aqua; Landsat 7; ETM+; Libya 4; pseudoinvariant calibration sites.

Paper 180549 received Jun. 29, 2018; accepted for publication Oct. 17, 2018; published online Nov. 2, 2018.

1 Introduction

Since their launch in 1999, Terra Moderate Resolution Imaging Spectroradiometer (MODIS) and Landsat 7 (L7) enhanced thematic mapper plus (ETM+) have been acquiring scientific measurements on a near-continuous basis. Both instruments were built by Raytheon, Santa Barbara Remote Sensing (SBRS), Goleta, California. Preflight calibration of both instruments was also performed at SBRS using a 100-cm spherical integrating source (SIS 100).[1,2] During the preflight calibration of these instruments, SBRS determined SIS radiances for multiple lamp levels. Furthermore, Butler et al.[3] led a radiometric measurement comparison of the SIS-100 used in these calibrations using transfer radiometers from different groups. The goal

*Address all correspondence to: Amit Angal, E-mail: amit.angal@ssaihq.com

1931-3195/2018/$25.00 © 2018 SPIE

of these measurements was to independently measure the radiance of SIS 100 and validate the assigned calibration uncertainties. Results showed that the SIS 100 radiances agreed with the transfer radiometer measurements to within ±3% in the visible/near-infrared (VNIR) region and ±4% in the short-wave infrared (SWIR) region for wavelengths not affected by atmospheric absorption.[3]

On-orbit, the Terra MODIS reflective solar bands (RSB) employ a reflectance-based calibration on the solar diffuser (SD) coupled with an SD stability monitor to track its degradation.[4] Terra MODIS also performs regular lunar measurements via its space-view port to track the sensor response change at an angle other than SD, therefore facilitating the characterization of the on-orbit changes in the response versus scan-angle (RVS).[5] Terra MODIS specified calibration uncertainty requirements are 2% in reflectance and 5% in radiance for the RSB at typical scene radiance levels and observations within ±45-SED scan angle range.[6] In the case of Terra MODIS, the SWIR bands have a serious thermal leak and electronic crosstalk effect that was identified during preflight calibration and has continued on-orbit. Although a correction algorithm has been formulated and implemented, noticeable effects are still observed in the level 1B (L1B) calibration product. With the exception of some short-wavelength ocean color bands, most RSB continue to meet the calibration uncertainty specification of 2%.[6,7]

On-orbit, the L7 ETM+ RSB also employs a suite of on-board calibrators that include internal calibrator lamps, the full aperture solar calibrator and a partial aperture solar calibrator. The calibration uncertainty specification for L7 ETM+ RSB is 5% in radiance at typical scene radiance levels.[2] Previously, the on-orbit calibration of L7 ETM+ was performed using a radiance-based calibration approach that relies on use of solar exoatmospheric irradiance values. After launch of the Landsat 8 (L8) Operational Land Imager (OLI), the on-orbit calibration approach for L7 ETM+ is based upon a NIST-traceable reflectance calibration (similar to Terra MODIS), with its calibration tied to OLI.[8]

As both instruments continue to operate well past their design lifetimes, the ability of the on-board calibrators to effectively monitor the two instruments' change on-orbit has diminished, particularly at short wavelengths. This was further reaffirmed from the temporal trending of the at-sensor reflectance from pseudoinvariant calibration sites (PICS).[9] In the case of Terra MODIS, the SD and lunar measurements provide insufficient information for an accurate on-orbit RVS characterization, particularly at short wavelengths, therefore resulting in a long-term reflectance drift as observed in the collection 5 level 1B (L1B) calibrated product. In the enhanced collection 6 (C6) L1B algorithm, the on-board calibrators are supplemented by the response trending from three North African PICS (Libya 1, Libya 2, and Libya 4) to provide more sampling across the scan-angle and therefore facilitate a better RVS characterization.[9] The results show an improved long-term stability of the top-of-atmosphere (ToA) reflectance trends for the Terra MODIS RSB, as reported by Doelling et al.[10] and Angal et al.[11] Similar to Terra MODIS, the L7 ETM+ long-term at-sensor reflectance over PICS is also monitored regularly and in 2012, a reflectance drift of up to 2.8% was observed in some RSB. As a result, the calibration gains for all ETM+ RSB were updated based on a weighted average of four individual PICS (Libya 4, Sudan 1, Mauritania 2, and Arabia 1). The entire ETM+ measurement dataset was reprocessed using these PICS-based gains, and mitigation in the reflectance drift was confirmed.[12]

In recent years, Saharan PICS have been widely used for on-orbit calibration, validation, and cross-calibration of satellite sensors. Cosnefroy et al.[13] performed the early work on the identification and characterization of Saharan PICS. Using this work as a baseline, the process of using PICS has evolved and matured over the last several years with improved accuracies and reduced uncertainties. Well-calibrated instruments like Tera MODIS and ETM+ rely on the temporal stability of PICS to correct for long-term drifts and inadequacies in their on-orbit calibration. Our previous work (Angal et al.[14]) evaluated the long-term reflectance stability for the spectrally matching bands of Terra MODIS and L7 ETM+ using the Libya 4 PICS. Long-term reflectance drifts, due to reasons discussed earlier, were observed at short wavelengths from the single site (Libya 4) that was used. Since this work, the on-orbit calibration methodologies for both instruments have significantly improved resulting in updated calibration versions. Landsat 7 ETM+ adopted a reflectance-based calibration tied to Landsat 8 OLI, and Terra MODIS adopted an improved RVS characterization using a combination of on-board and Earth view measurements.

In this paper, the reflectance drifts for the spectrally matching RSB of these instruments, with the most recent calibration version (collection 6.1 for Terra MODIS and collection 1 for L7 ETM+), over Libya 4 and three other PICS (Niger 1, Niger 2, and Libya 1) are evaluated. In comparison with the previous work, improved corrections for bidirectional reflectance distribution function (BRDF) and characterization of atmospheric effects are presented in this paper. A semiempirical model (Roujean et al.[15]) is implemented to remove the effects for surface BRDF effects. Overall, the reflectance drifts from the four sites at all wavelengths are less than 2% with site-dependent uncertainties. This is an expected result for the Libya 4 and Libya 1 PICS that have been used in the on-orbit calibration of the two instruments, and the results from Niger 1 and Niger 2 further reaffirm the improvements.

For satellites flying in the same orbit, as is the case with L7 and Terra, near simultaneous views of stable ground targets, such as PICS, facilitate a unique opportunity to evaluate the absolute calibration differences between the two instruments. Only the same-day scenes (~30- min overpass time difference) with BRDF-normalized reflectances are used in this study. It is necessary to account for the differences between the relative spectral responses (RSR) for the spectrally matching bands. In this paper, this process is performed using hyperspectral observations from Earth observing 1 (EO-1) Hyperion and radiative transfer simulations using MODTRAN.[16,17] The effects for atmospheric water-vapor absorption are evaluated using radiative transfer simulations and real-time measurements via the NCEP/NCAR database.[18] These corrections are derived for each PICS considered in this study. The results from each PICS indicate that the reflectance difference between Terra MODIS and Landsat 7 ETM+ spectrally matching bands, after all the above-mentioned corrections, agrees to within 4% for most bands. This trend is generally consistent with that observed during the round-robin preflight calibration comparison performed by Butler et al.[3] A vital aspect of any cross-sensor comparison is a comprehensive uncertainty analysis and an in-depth assessment of the uncertainties from the PICS-based approach is discussed in this paper. Furthermore, the methodologies discussed in this paper will be extended in the future to evaluate the on-orbit calibration agreement between L8 OLI and Aqua MODIS, and Visible Infrared Imaging Radiometer Suite (VIIRS) instrument on Suomi NPP and NOAA-20 satellites.

2 Site and Sensor Overview

2.1 *Site Overview*

The PICS in the North African region are popularly used in on-orbit calibration and validation for various satellite sensors in the reflective solar region. Following up on Cosnefroy et al.[13] work, Lachérade et al.[19] performed a comprehensive study of these sites using satellite observations. As introduced earlier, out of the 20+ African PICS, four sites namely, Libya 1, Libya 4, Niger 1, and Niger 2 were chosen for this cross-calibration work. Figures 1(a)–1(d) show L7 ETM+ images of these sites. The Infrared and Visible Optical Sensors Working Group from the Committee of Earth Observing Satellites has recognized the importance of the desert sites for instrument calibration and as a part of that work, Lachérade et al.[19] also identified usable areas

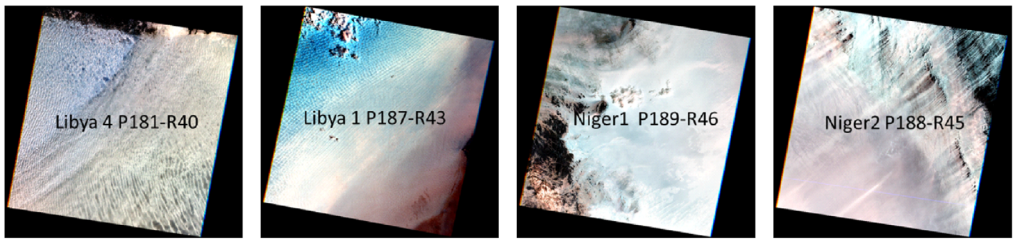

Fig. 1 L7 ETM+ images for the chosen PICS. (a) Libya4 P181-R40, (a) Libya1 P181-R43, (a) Niger1 P189-R46, and (d) (a) Niger2 P188-R45.

Table 1 PICS RoI bounding box (in deg).

Site	Min-lat	Max-lat	Min-lon	Max-lon
Libya 4	28.45	28.65	23.29	23.49
Libya 1	24.40	24.60	13.20	13.40
Niger 1	19.75	19.95	9.9	10.10
Niger 2	21.00	21.20	10.50	10.70

(0.9 deg×0.9 deg) for these sites, as listed in Table 1. Each of these sites shows varying characteristics in terms of surface reflectance, atmospheric variations, spatial and spectral homogeneity, etc. However, it should be noted that, with a 30-min (or less) difference between the overpass times of the two satellites, uncertainties due to atmospheric variations, spatial and spectral inhomogeneity should be minimized significantly. A detailed discussion of the uncertainties associated with this cross-calibration is also discussed in the latter sections.

2.2 *Sensor Overview*

The design and on-orbit performance of the ETM+ and MODIS instruments has been extensively documented by Xiong et al.[20] and Markham et al.[21] Some key details related to the spectral and spatial characteristics that are relevant to this work have been listed in Table 2. It is noteworthy that the ETM+ bands have a wider bandpass and a finer spatial resolution compared to the corresponding spectrally matching bands of MODIS. The large uniform areas chosen from the PICS help reduce the uncertainties due to mismatches in the spatial resolutions during the computation of mean reflectance or radiance of the chosen region-of-interest (RoI). The mismatch in the spectral bandwidths between the two sensors is the primary source for the observed differences in the ToA reflectance between the two instruments. Hyperspectral measurements of ToA reflectance of the ground target have been previously used to account for this mismatch, and the uncertainty associated with such corrections has also been well documented.[22] In this work, the ToA reflectance measurements from EO-1 Hyperion are used to account for the spectral mismatch between ETM+ and Terra MODIS RSB. Launched in November 2000, in the same orbit as Terra and L7, the EO-1 mission acquired successful observations of the Earth via Hyperion and advanced land imager instruments. The EO-1 satellite was decommissioned in the early months of 2017 after several years of a gradual deorbiting. On-orbit calibration performance of the EO-1 Hyperion has been previously reported.[23,24]

Table 2 Summary of the spectral bandwidth (BW), center wavelength (CW), and spatial resolution.

	Terra MODIS			L7 ETM+			
Band	BW (μm)	CW (μm)	Spatial resolution (m)	Band	BW (μm)	CW (μm)	Spatial resolution (m)
1	0.62–0.67	0.64	250	3	0.63–0.69	0.66	30
2	0.84–0.87	0.85	250	4	0.77–0.90	0.83	30
3	0.45–0.47	0.46	500	1	0.45–0.51	0.47	30
4	0.54–0.56	0.55	500	2	0.52–0.60	0.56	30
6	1.62–1.65	1.62	500	5	1.55–1.75	1.65	30
7	2.10–2.15	2.11	500	7	2.09–2.35	2.20	30

3 Methodology

This section discusses in detail the various steps involved with the cross-calibration methodology. The summary of the steps involved is shown in Fig. 2.

1. For each of the four PICS, all available scenes of ETM+ and MODIS were identified using the search tools provided on the EarthExplorer and LAADS websites.[25,26] The level-1 calibrated products providing the ToA radiance and reflectance were archived. The collection 1 products were used for ETM+ and collection 6.1 products for Terra MODIS. Only same-day scenes were used. The PICS scenes are at-nadir with a repeat cycle of 16 days.
2. The ETM+ products are obtained in a GeoTiff format with the Universal Transfer Mercator (UTM) projection applied. The Terra MODIS level 1B (L1B) products are only corrected for radiometric effects; the MODIS Swath Reprojection Tool (MRTSwath) geometric correction was used to apply the ETM+ map projection to the MODIS L1B products.[27]
3. The pixels corresponding to the RoI specified in Table 1 are used to compute the mean ToA statistics for each spectral band. In the case of Terra MODIS, the statistics are computed at the native spatial resolution for each band (250 or 500 m). Furthermore, the brightness temperature (BT) is also computed for the 11-μm channel on each instrument (band 6 for ETM+ and band 31 for Terra MODIS). As the two instruments have different spatial resolutions, ground spatial structures can induce some variations that were generally observed to be within 1.2% and consistent over time. More discussion related to uncertainties associated with spatial characteristics is discussed in Sec. 4.5.
4. The mean at-sensor reflectance time-series for each band from the same-day scenes is further assessed to identify the scenes impacted by clouds, saturation, etc. The following steps were undertaken to identify these scenes.

    a. The use of atmospheric window channels was previously used to discriminate the BT of cloud pixels with the BT from hot desert pixels.[28] The BT retrieved by the atmospheric window channels (11 and 12 μm) over the hot Libyan desert typically exceeds 300 K. Also, the MODIS cloud-mask product has a restoral test that classifies a desert scene as "confidently clear" if the BT for band 31 (11 μm) exceeds 302.5 K.[29] Therefore, any scene-pair where the mean BT for the RoI from either instrument is below 300 K is eliminated from further analysis.

    b. The above test eliminates the scenes whether the entire or a majority of the scene is covered by clouds. The scene-pairs where clouds are impacted for certain pixels of

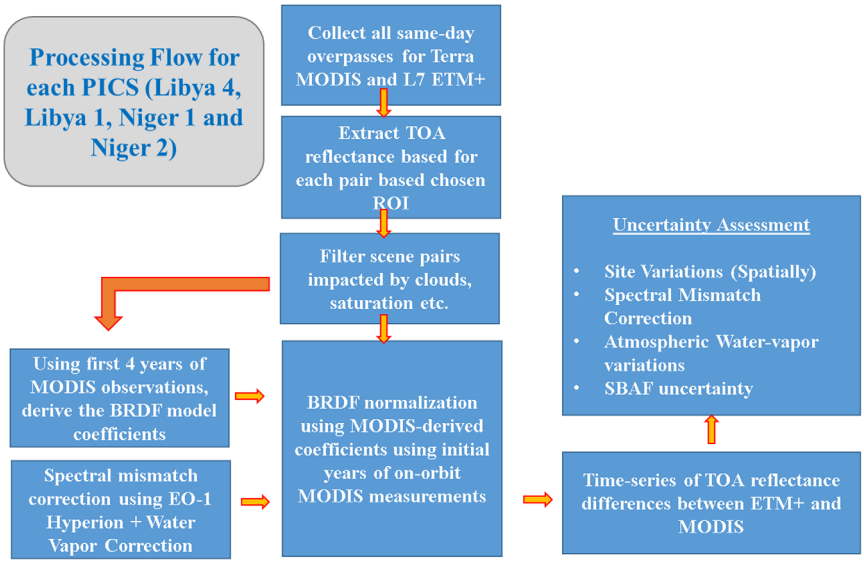

Fig. 2 Flowchart of the cross-calibration methodology.

the RoI also need to be identified. In the case of Terra MODIS, the MODIS cloud-mask product, which provides pixel level classification for clouds, was employed to identify and retain scenes that have greater than 75% of the pixels flagged as "confidently clear."

c. The scene-pairs where saturation in the instrument response while viewing the desert is observed in either instrument is also eliminated.

5. The filtered at-sensor reflectance time-series from Terra MODIS is used to derive the BRDF normalization coefficients on a per-band basis. Differences in directional observations due to solar and sensor view geometries and overpass times induce surface and atmospheric BRDF impacts on the retrieved ToA reflectance. Due to the complexity associated with a physical BRDF model, a simple kernel-driven model replying on the weighted sum of the geometric and volumetric functions of the view and illumination geometry and an isotropic parameter was chosen to determine the modeled reflectance.[13] All near-nadir observations of Terra MODIS RSB from the first 4 years were used to derive these BRDF normalization coefficients by minimizing the residual error using an optimization algorithm. The per-band BRDF normalization coefficients from Terra MODIS are applied to the corresponding spectrally matching bands of ETM+ to retrieve the corresponding ETM+ time-series post-BRDF correction.
6. As introduced earlier, the mismatch due to differing RSRs between the two instruments is corrected using hyperspectral measurements from EO-1 Hyperion. The Level 1G images of EO-1 Hyperion for each PICS were archived and processed. Hyperion has a very narrow swath (7 km) in comparison with MODIS and ETM+, so all pixels within the specified RoI were chosen to calculate the ToA reflectance across the 196 channels from 0.4 to 2.2 μm. The EO-1 Hyperion data product provides an at-sensor radiance that is converted to ToA reflectance using a solar irradiance spectra from Chukur.[13] The derivation of spectral band adjustment factor (SBAF), as formulated by Chander et al.,[22] to account for the RSR differences was calculated for every Hyperion scene. Consequently, a time-series of SBAF for each band-pair was obtained. Due to the varying orbit of the EO-1 satellite, same-day Hyperion scene pairs were not available. A lifetime average of SBAF temporal trending is used to derive the correction for each scene-pair of MODIS and ETM+. Also, an additional correction for the columnar atmospheric variations, specifically for L7 ETM+ bands 4 and 5, is accounted for via an additional correction discussed in later sections.

4 Results

4.1 *ToA Reflectance*

Using the methodology described in the earlier section, the time-series of ToA reflectance is generated on a per-band basis for each of the four sites. Figure 3 shows the mean ToA reflectance trending for the four sites for the spectrally matching bands around 0.64 μm. The error bars denote the 1-sigma deviation of the ToA reflectance around the mean value. Figure 4 shows the mean ToA reflectance trending for the spectrally matching bands centered at 0.86 μm. The data shown in Figs. 3 and 4 are all available overpasses from L7 ETM+ over the given site and all available near-nadir overpasses for Terra MODIS. During the first decade of L7 ETM+ operations, the data from the Niger sites were not collected as frequently as the Libyan sites, therefore leading to some temporal gaps in the data. In the case of Terra MODIS, the near-nadir collects are at a frequency of one every 16 days therefore leading to a more continuous time-series of collects. Figure 5 shows the lifetime mean ToA reflectance plotted as a function of wavelength for all four sites. The solid lines denote the L7 ETM+ reflectance, and the dotted lines denote the Terra MODIS reflectance. Overall, the reflectance from the Niger 2 site is seen to be the lowest across all wavelengths. The major cause behind the deviation of the ToA reflectance ratio between L7 ETM+ and Terra MODIS shown in Fig. 5(b) is the RSR mismatch between the two instruments, especially at the longer wavelengths (beyond 0.8 μm).

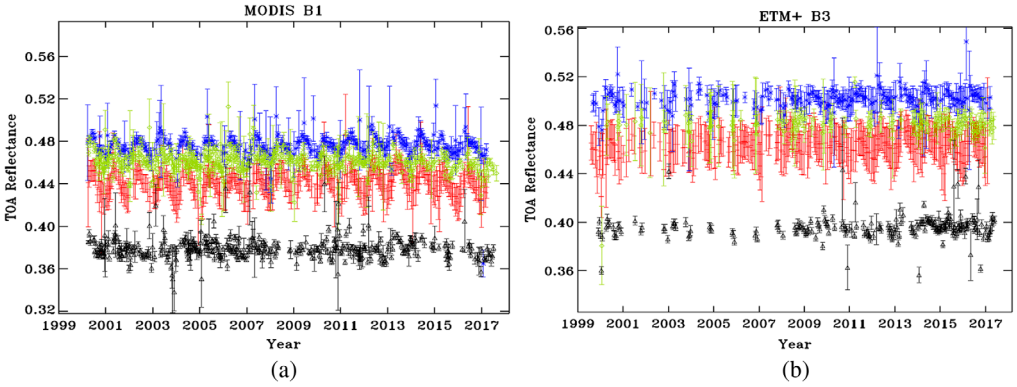

Fig. 3 ToA reflectance trending for the (a) 0.64 μm channels of Terra MODIS and (b) L7 ETM+: Libya 4 (red), Libya 1(blue), Niger 1 (green), and Niger 2 (black).

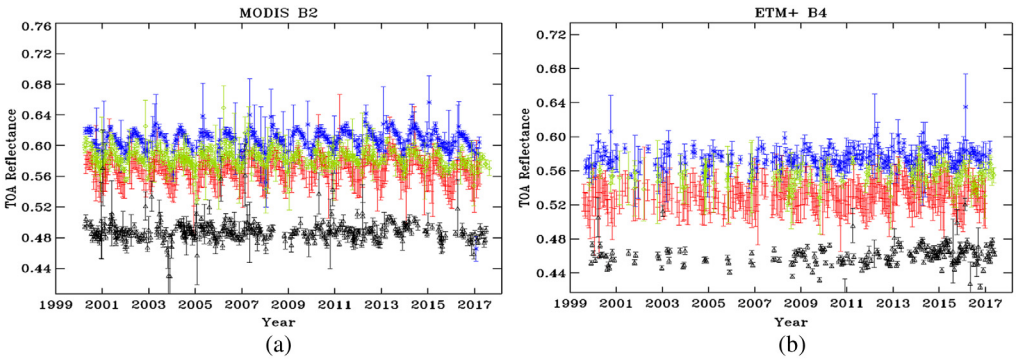

Fig. 4 ToA reflectance trending for the (a) 0.86 μm channels of Terra MODIS and (b) L7 ETM+.

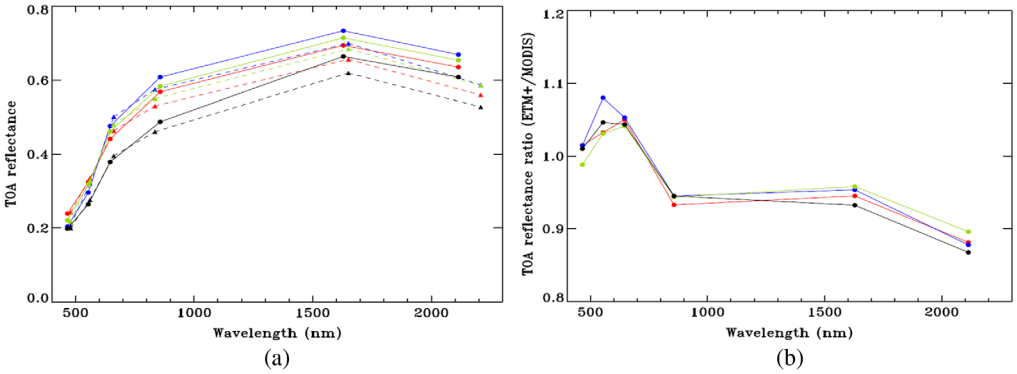

Fig. 5 (a) Mean ToA reflectance versus wavelength, the solid lines denote L7 ETM+ reflectance and the dotted lines denote the MODIS reflectance, and (b) ToA reflectance ratio.

The yearly oscillations in the ToA reflectance trends are predominantly caused due to the surface and atmospheric BRDF effects. Although impacting both instruments, it is more evident in the Terra MODIS trends due to a continuous time-series of reflectance trend. The BRDF normalized reflectances are used to evaluate the long-term drifts in each of the spectral bands, and the results are presented in the next subsection.

4.2 *Long-Term Drift*

The BRDF coefficients derived from the first few years of Terra MODIS observations are used to normalize the time-series reflectances for both instruments. Only the same-day scenes after

filtering for clouds, saturation, etc. are retained for further processing. The derived coefficients are site-specific as well as band-dependent. Figure 6 shows the Libya 4 measured ToA reflectances normalized by the BRDF model reflectances for Terra MODIS bands 1 and 2 with the spectrally matching ETM+ bands 3 and 4. The seasonal trend in the ToA reflectance trend as observed in Figs. 3 and 4 is reduced from 7% to within 3% for Terra MODIS band 1. In the case of Terra MODIS band 2 and ETM+ band 4, the improvement is not as pronounced due to the water-vapor absorption feature in the ETM+ RSR. The BRDF normalized time-series is normalized to the mission beginning to estimate the long-term drift on a band-by-band basis. A simple linear model is used to estimate the cumulative long-term reflectance drift from 2000 to 2017, and the standard error around the linear fit is also calculated. A similar technique is applied for all the band pairs from each of the four sites and the long-term drift from each site is shown as a function of wavelength in Fig. 7. With the exception of one case (ETM+ band 3 from Niger 1),

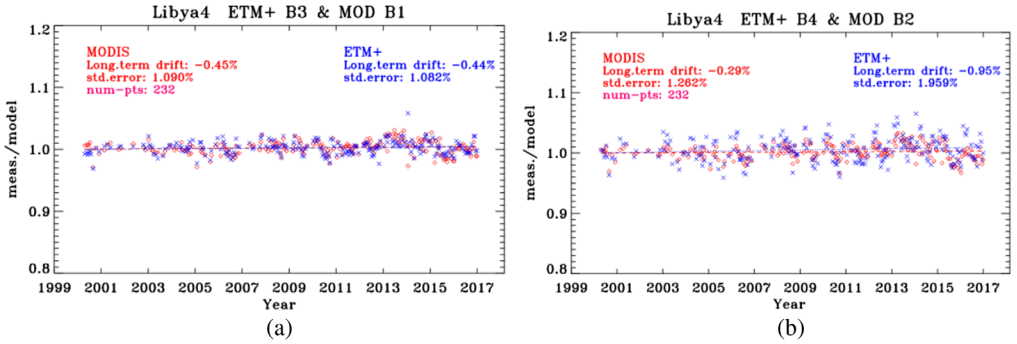

Fig. 6 BRDF normalized ToA reflectance for (a) ETM+ band 3 and MODIS band 1 and (b) ETM+ band 4 and MODIS band 2.

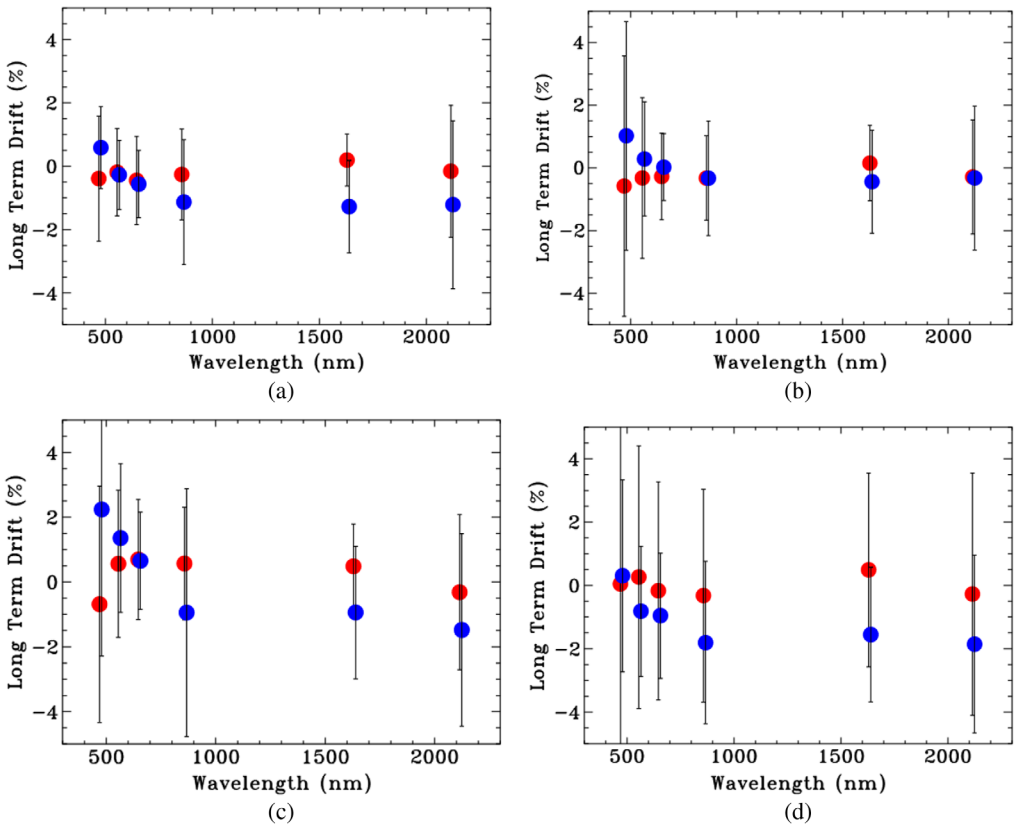

Fig. 7 Long-term drift for ETM+ (blue) and MODIS (red) from 2000 to 2017 for (a) Libya 4, (b) Libya 1, (c) Niger 1, and (d) Niger 2

the long-term drift from all sites is within ±2%. Larger standard error values are observed for the Niger sites in comparison with the Libyan sites. A major reason for this is the fewer number of ETM+ scenes (and hence a reduced number of scene-pairs) over the Niger 1 and Niger 2 sites.

4.3 *SBAF Correction*

As introduced earlier, hyperspectral measurements of the ground site were obtained using EO-1 Hyperion. In contrast to the Terra MODIS and Landsat 7 ETM+ swaths, EO-1 Hyperion has an extremely small swath of 7 km and hence, it does not cover the entire RoI selected for each site. Consequently, a smaller RoI (within the larger RoI) was selected to derive the ToA reflectance from each Hyperion overpass. While over 400+ EO-1 Hyperion scenes were available over Libya 4 and Libya 1, less than 50 scenes were available over the Niger sites. Also, no Hyperion scenes over the Libyan or Niger sites were available before 2004. Figure 8(a) shows the lifetime average ToA reflectance profile from all available EO-1 Hyperion scenes over each site. The reflectance profile, at 10-nm spectral sampling, provides a convenient mechanism to account for the spectral mismatch between the two RSRs. Using this information and the RSRs for ETM+ and MODIS, the SBAF is computed and is shown in Fig. 8(b). The trend of the SBAF curve is similar to the ETM+/MODIS reflectance ratio, as shown in Fig. 5(b). This further reaffirms the fact that a dominant source of the deviation in the ratios observed in Fig. 5(b) is caused due to the spectral mismatch between the two instruments. The SBAF shown in Fig. 8(b) is applied to the BRDF normalized ToA reflectances to obtain the differences between the two instruments.

The chosen PICS are known to exhibit excellent radiometric, spatial, and spectral stability, and a stable long-term trending of the SBAF further reaffirms it.[30] However, due to the differing orbits, an L7 ETM+ and Terra MODIS scene-pair is not necessarily coupled with an EO-1 Hyperion overpass, therefore restricting the ability to characterize the localized scene conditions. This is especially critical for ETM+ band 4 and band 5 that have a water-vapor absorption feature in their RSR that is absent from the corresponding Terra MODIS bands 2 and 6.

In order to evaluate the impact of the water-vapor absorption feature on the estimate of RSR mismatch, a mid-latitude desert spectrum generated using MODTRAN was varied against different amounts of column atmospheric water-vapor to estimate the variation of SBAF, as shown in Fig. 9(a). Significant variation (up to 8%) is observed in the SBAF as a function of water-vapor for ETM+ band 4/Terra MODIS band 2 and ETM+ band 5/Terra MODIS band 6 pairs. Figure 9(b) shows the columnar atmospheric retrieved as a part of the SDSU Image Processing Lab's Atmospheric Modelling database. This database was developed to facilitate atmospheric correction of satellite imagery and houses three key inputs: aerosol, water-vapor, and ozone on a global scale. The water-vapor information is ingested from the NOAA NCEP and provides measurements on a time-scale of every 3 h over a given ground target (PICS in this case). For every overpass, the retrieved water-vapor from Fig. 9(b), along with the curve shown in Fig. 9(a), is used to compute an equivalent time-dependent correction factor that is used with the SBAF to correct the BRDF normalized reflectances.

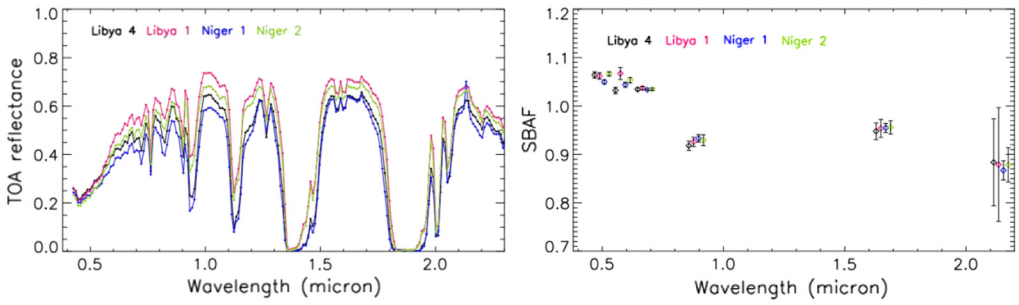

(a) (b)

Fig. 8 (a) Lifetime averaged ToA reflectance spectrum for the four sites from EO-1 Hyperion. (b) Lifetime average SBAF derived for the spectrally matching bands of ETM+ and MODIS.

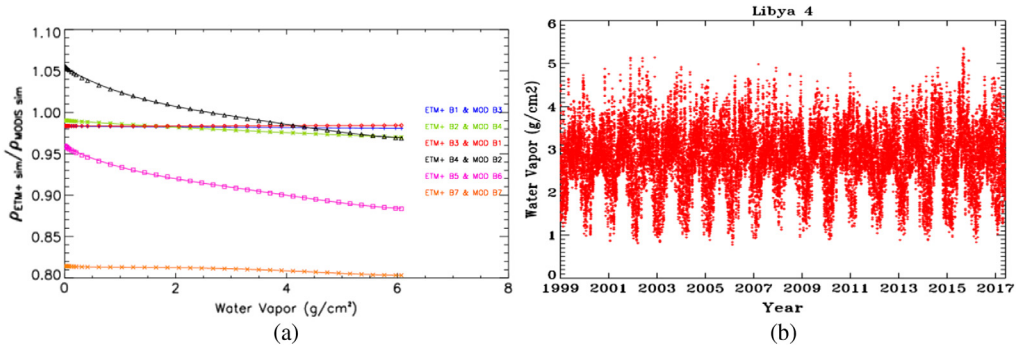

Fig. 9 (a) SBAF dependence on columnar atmospheric water-vapor as simulated using MODTRAN and (b) columnar atmospheric water-vapor over Libya 4.[18]

4.4 *Reflectance Differences*

Using the SBAF that includes a time-dependent water-vapor correction, the BRDF normalized reflectances are corrected and shown in Fig. 10. The BRDF normalized reflectances for Libya 4 before SBAF and water vapor correction are plotted in pink and after SBAF and water vapor correction are plotted in purple. The deviation of these time-trends (post BRDF and SBAF

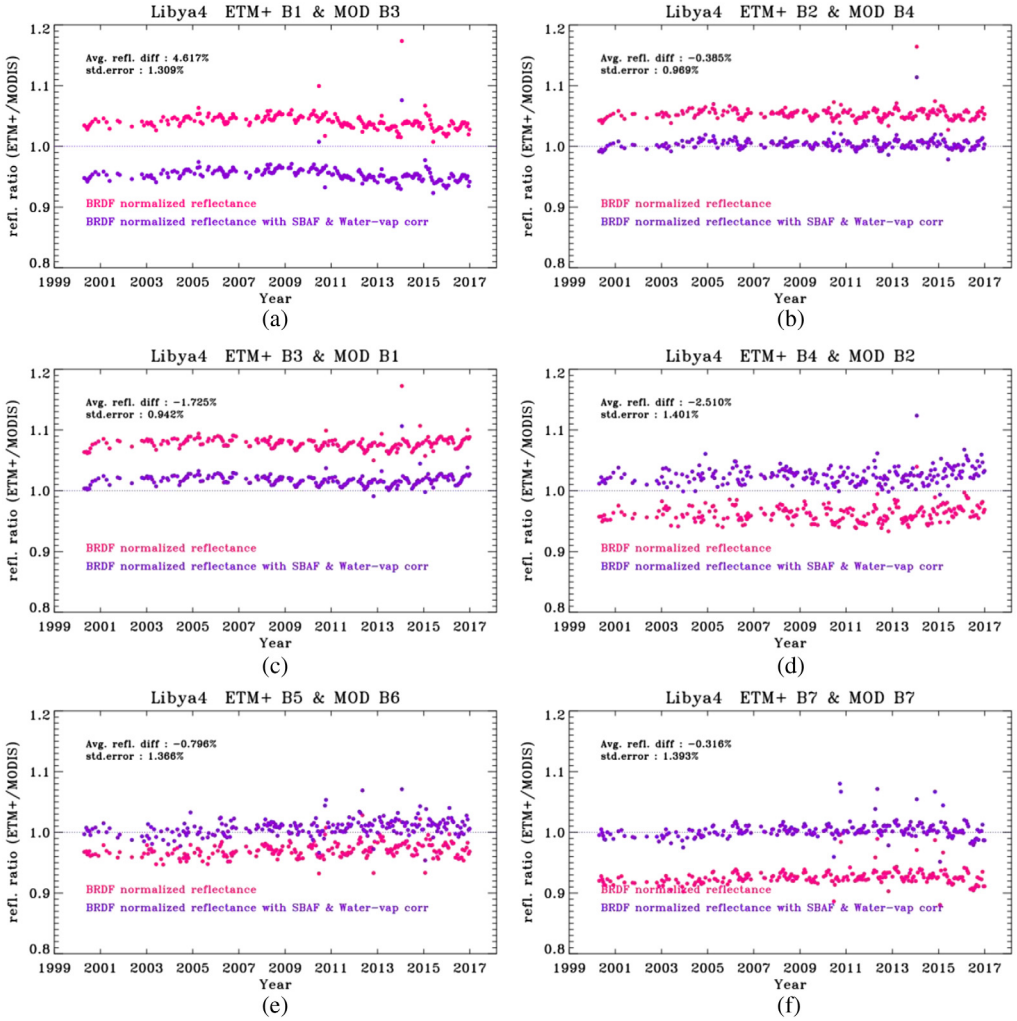

Fig. 10 (a)–(f) L7 ETM+ and Terra MODIS reflectance differences for Libya 4 before and after SBAF and water-vapor correction.

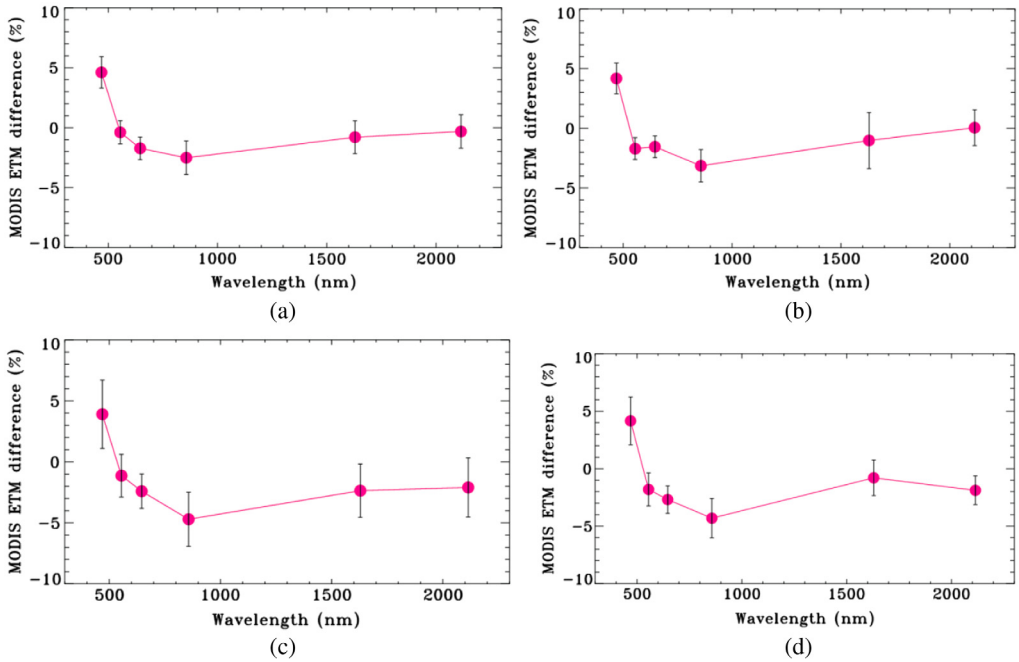

Fig. 11. Summary of the reflectance differences between MODIS and ETM+ from four PICS: (a) Libya 4 (b) Libya 1 (c) Niger 1, and (d) Niger 2.

correction) from unity represents the reflectance differences between the two instruments. Similar corrections are also applied for the other three PICS. An overcorrection is seen for ETM+ band 1 and MODIS band 3, where the reflectance ratio (~1.03) is reduced (to around 0.96) postcorrection. This overcorrection is caused due to the limitation of the Hyperion-based SBAF correction and is discussed in further detail in the next section. ETM+ band 2 and MODIS band 4 show an excellent agreement to within 0.3%. In the case of ETM+ band 3 and MODIS band 1, the agreement is within 2%. The ETM+ band 4 and MODIS band 2 agree within 3% and the SWIR bands show an excellent agreement to within 2%. In the case of ETM+ bands 4 and 5, the additional correction for water-vapor has been applied to these ratios and, as a result, reduced fluctuations are observed in the corrected (purple) trends in comparison with the uncorrected (pink) trends.

A lifetime average of the BRDF normalized and SBAF, water-vapor corrected reflectances, and its standard error is computed for each band-pair and every PICS. Figure 11 shows the summary for all four sites. A large disagreement (of about 5%) is observed for the shortest wavelength band across all the four PICS. At other wavelengths, the agreement is generally within ±2%. In comparison with the Libyan sites, a greater standard error is observed for the Niger 1 and Niger 2 results.

4.5 *Discussions*

The disagreement between ETM+ band 1 and MODIS band 3, observed for all the PICS, is investigated further in this section. The coarsely sampled (10 nm) EO-1 Hyperion reflectance spectra are compared with the finely sampled spectra from ENVISAT scanning imaging absorption spectrometer for atmospheric CARTOGRAPHY (SCIAMACHY) in Fig. 12(a). The ENVISAT SCIAMACHY mission (March 2002 to April 2012) produced high spectral resolution (0.2 to 1.5 nm) data over the wavelength range from 240 to 1700 nm and in select spectral bands around 2 and 2.4 μm.[31] Doelling et al.[32] demonstrated the use of SCIAMACHY to derive SBAFs between MODIS and other various GEO/LEO sensors and more recently, Scarino et al.[33] have incorporated SCIAMACHY as the primary source to derive the SBAFs via a web-based tool. As shown in Fig. 12, the SCIAMACHY spectrum is very finely sampled, especially within the Terra MODIS spectral bandpass. Furthermore, the SBAF computed from the SCIAMACHY spectrum

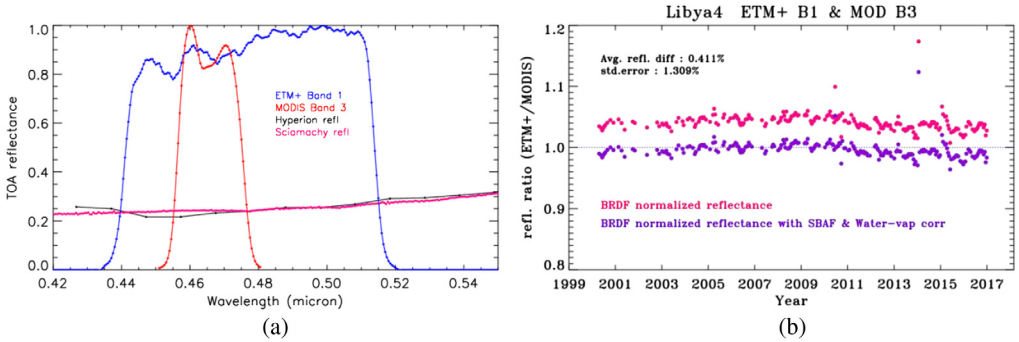

Fig. 12 (a) ToA reflectance profile comparison between SCIAMACHY and Hyperion and (b) its impact on the cross-calibration results.

of Libya 4 from Fig. 12(a) results in a value of 1.019 instead of 1.064 (from Hyperion). The BRDF normalized reflectances shown earlier were corrected using the SCIAMACHY-based SBAF, and the results are shown in Fig. 12(b). The 4.23% overcorrection observed with the Hyperion SBAF is essentially eliminated and the difference between the two sensors is observed to be within 0.5% with a standard error of 1.3%. This result confirms that the difference observed for ETM+ band 1 and Terra MODIS band 3 was a result of the limitation of the EO-1 Hyperion spectrum. Ideally, a high-resolution spectrum such as produced by ENVISAT SCIAMACHY should be used to compute the SBAF; however, all the SCIAMACHY data to produce such information were not available for this work.

The RoIs selected for each of the PICS are based of the work done by Lachérade et al.[19] More recently, Kaewmanee et al.[34] have formulated and implemented a PICS normalization process to bring various PICS on the same scale based on a common reference. As part of this effort, the CNES RoIs were evaluated based on the ToA measurements from the well calibrated L8 OLI. Based on these measurements, a revised (optimal) RoI that has a 3% spatial, spectral, and temporal stability has been identified for each of these PICS. Figure 13 shows a comparison between the baseline CNES ROI and optimal RoI chosen from the above work. Ideally, for stable radiometric targets, such as PICS, variations in the RoI are expected to have minimal impacts on the derived results; however, if the optimal RoI produces an improved spatial, spectral, and temporal stability, an improvement in the results is generally expected. The cross-calibration process described earlier was performed using the optimal RoIs and the results were compared with those obtained from the baseline RoI. Figure 13 shows a comparison of cross-calibration results using both RoIs for Niger 1.

4.6 *Uncertainty Analysis*

To address the uncertainty associated with this cross-calibration, it is convenient to divide the approach into three parts: (1) the uncertainties associated with the individual PICS used in this

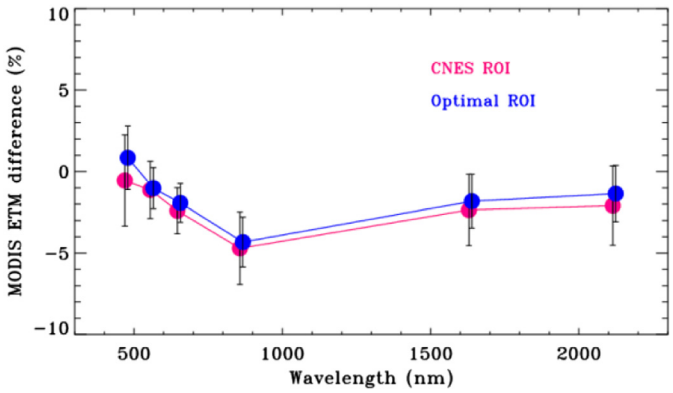

Fig. 13 MODIS ETM+ reflectance difference using the CNES specified and the optimal RoI.

analysis; (2) the calibration uncertainty of the sensors; (3) and the uncertainty due to the spectral bandpass differences of the two sensors. The uncertainties due to the PICS that were used in this study are fairly well understood. Previous analyses of these sites using 4 years of Landsat 8 data have indicated that the overall temporal uncertainties were less than 2.3% for all spectral bands and for all four sites.[34] These characterizations include both the surface and atmosphere as a combined measure of the overall uncertainty of the site. For the Landsat 7 sensor, analyzed over a longer period of time, the overall uncertainties of these PICS were less than 2% for all the bands for both sensors, with the exception of Libya1 in the blue bands (ETM+ band 1 and MODIS band 3) and Libya4 in the SWIR2 (band 7) bands, which exhibit, respectively, 2.7% and 2.4%. The overall range of values is shown in the first entry of Table 3. As for Terra MODIS, the largest temporal uncertainties were for the Niger2 and Niger1 Blue band, and the Niger1 SWIR2 band, which were 2.9% and 2.1%, respectively. The total range of the uncertainties for MODIS is given in the second entry of Table 3. The overall calibration uncertainty for Landsat 7 is 5%.[2] Similarly, Terra MODIS has a calibration uncertainty in the VNIR bands of 2% and in the SWIR bands of 3%.[7] These data are also shown in Table 3. The uncertainty due to spectral differences between the two sensors was determined by an analysis of 14 years of hyperspectral data obtained by Hyperion. By analyzing the standard deviation about the mean spectral values for each of the sites, it was found that uncertainties due to spectral difference ranged from 0.1% to 1.8%, less than 1.05% for VNIR and ranging from 0.9% to 1.8% for SWIR bands. This information is also shown in Table 3. Combining these three sources of uncertainty together, with the reasonable assumption that they are uncorrelated, results in an overall range of uncertainty for the cross-calibration from 5.6% to 6.8% with the largest uncertainty occurring in the SWIR 2 band due to large spectral bandpass differences between the sensors as well as the significant water absorption features that exist at these wavelengths. For completeness, the uncertainties are broken out by site and spectral band in Table 4, and so, the reader can ascertain relative differences between the sites and wavelengths.

Table 3 Summary of cross-calibration Landsat7 and Terra MODIS uncertainty sources.

Uncertainty sources	Uncertainty (%)	Remarks
Landsat7 PICS temporal uncertainty	0.85%–2.70%	All bands and all for four PICS
Terra MODIS PICS temporal uncertainty	0.74%–2.90%	All bands and all for four PICS
Landsat 7 calibration uncertainty	5%	All bands
Terra MODIS calibration uncertainty	2%–3%	2% for VNIR and 3% for SWIR bands
SBAF calculation uncertainty	0.1%–1.8%	Within 1.05% for VNIR and 0.9% to 1.8% SWIR bands
Total	5.6%–6.8%	All bands and all for four PICS

Table 4 Landsat7 ETM+ and Terra MODIS cross-calibration total uncertainty analysis for all four PICS.

Total uncertainties	Libya1	Libya4	Niger1	Niger2
Blue	6.4%	5.6%	6.3%	6.3%
Green	5.8%	5.6%	5.8%	5.9%
Red	5.6%	5.6%	5.6%	5.7%
NIR	5.8%	5.9%	5.9%	6.0%
SWIR1	6.1%	6.1%	6.2%	6.1%
SWIR2	6.4%	6.7%	6.6%	6.8%

5 Conclusion

Using near-simultaneous scene-pairs from PICS is an effective way to perform sensor cross-calibration. In this work, L7 ETM+ and Terra MODIS instruments, that are independently calibrated prelaunch and postlaunch, utilize PICS to perform a reflectance-based cross-calibration of their spectrally matching RSB. Utilizing the excellent temporal stability of PICS, long-term calibration stability of each RSB of both instruments is evaluated independently. Our previous work developed the initial methodology for this cross-calibration that has now been expanded to apply to a longer-time series from multiple ground sites, including an in-depth analysis of the associated uncertainties. The latest versions of calibrated data (collection 6.1 for MODIS and collection 1 for ETM+) are used in this work. Both instruments demonstrate an excellent temporal stability with the long-term drifts for all bands well within 2% over 18 years. As expected, site-to-site variations in the results are observed with the Libyan sites showing lower standard error compared to the Niger sites. To minimize the impacts of the short-term and long-variations associated with the site, only same-day scenes are chosen to evaluate the at-sensor reflectance differences between spectrally matching bands. Although the effects of site and atmosphere BRDF are minimal, a MODIS-based semiempirical model is used to derive the correction coefficients that are applied to the spectrally matching ETM+ bands. EO-1 Hyperion based SBAF correction and use of near real-time water-vapor information are employed to account for the spectral mismatch between the RSRs to get an agreement within $\pm 4\%$ (from the Libyan sites) for all bands except for the short wavelength ETM+ band 1 and MODIS band 3. The difference at short wavelengths is due to the limitation of the EO-1 Hyperion to provide sufficient spectral sampling at these wavelengths. The use of SCIAMACHY is used to confirm this. A detailed uncertainty characterization including the site variability and on-orbit behavior of the instruments has also been performed. The combined uncertainty budget for the cross-calibration between ETM+ and MODIS RSB using the PICS ranges from 5.6% to 6.8%. The techniques developed here can be extended to assess near-simultaneous measurements from other EO sensors such as Aqua MODIS, L8 OLI, and SNPP VIIRS, which are follow-on missions to Terra MODIS and Landsat 7 ETM+.

Acknowledgments

The authors would like to thank Gyanesh Chander and Taeyoung Choi for their efforts during the initial development of this collaborative effort. The authors would also like to thank Aisheng Wu and other members of the MODIS characterization support team that have supported this effort in some way or the other. The SCIAMACHY profile for Libya 4 was provided by Ben Scarino, SSAI.

References

1. W. Barnes, T. S. Pagano, and V. Salomonson, "Prelaunch characteristics of the moderate resolution imaging spectroradiometer (MODIS) on EOS-AM1," *IEEE Trans. Geosci. Remote Sens.* **36**(4), 1088–1100 (1998).
2. B. L. Markham et al., "Landsat-7 enhanced thematic mapper plus radiometric calibration," *Can. J. Remote Sens.* **23**(4), 318–332 (1997).
3. J. Butler et al., "Radiometric measurement comparison on the integrating sphere source used to calibrate the moderate resolution imaging spectroradiometer (MODIS) and the Landsat 7 enhanced thematic mapper plus (ETM+)," *J. Res. Nat. Inst. Stand. Technol.* **108**(3), 199–228 (2003).
4. X. Xiong et al., "MODIS on-orbit calibration and characterization," *Metrologia* **40**(1), S89–S92 (2003).
5. J. Sun et al., "MODIS reflective solar bands on-orbit lunar calibration," *IEEE Trans. Geosci. Remote Sens.* **45**(7), 2383–2393 (2007).
6. X. Xiong et al., "Terra and aqua MODIS calibration algorithms and uncertainty analysis," *Proc. SPIE* **5978**, 59780V (2005).

7. X. Xiong et al., "Updates of MODIS on-orbit calibration uncertainty assessments," *Proc. SPIE* **10402**, 104020M (2017).
8. E. Micijevic, Md. O. Haque, and N. Mishra, "Radiometric calibration updates to the Landsat collection," *Proc. SPIE* **9972**, 99720D (2016).
9. J. Sun et al., "Time-dependent response versus scan angle for MODIS reflective solar bands," *IEEE Trans. Geosci. Remote Sens.* **52**(6), 3159–3174 (2014).
10. D. R. Doelling et al., "The radiometric stability and scaling of collection 6 terra- and aqua-MODIS VIS, NIR, and SWIR spectral bands," *IEEE Trans. Geosci. Remote Sens.* **53**(8), 4520–4535 (2015).
11. A. Angal et al., "Impact of Terra MODIS collection 6 on long-term trending comparisons with Landsat 7 ETM+ reflective solar bands," *Remote Sens. Lett.* **4**(9), 873–881 (2013).
12. J. A. Barsi et al., "Landsat-7 ETM+ radiometric calibration status," *Proc. SPIE* **9972**, 99720C (2016).
13. H. Cosnefroy, M. Leroy, and X. Briottet, "Selection and characterization of Saharian and Arabian desert sites for the calibration of optical satellite sensors," *Remote Sens. Environ.* **58**(1), 101–114 (1996).
14. A. Angal et al., "Multitemporal cross-calibration of the Terra MODIS and Landsat 7 ETM+ reflective solar bands," *IEEE Trans. Geosci. Remote Sens.* **51**(4), 1870–1882 (2013).
15. J. L. Roujean, M. J. Leroy, and P. Y. Deschamps, "A bidirectional reflectance model of the Earth's surface for the correction of remote sensing data," *J. Geophys. Res.* **97**(D18), 20455–20468 (1992).
16. J. Pearlman et al., "Hyperion, a space-based imaging spectrometer," *IEEE Trans. Geosci. Remote Sens.* **41**(6), 1160–1173 (2003).
17. A. Berk et al., "MODTRAN 5: a reformulated atmospheric band model with auxiliary species and practical multiple scattering options: update," *Proc. SPIE* **5806**, 662–667 (2005).
18. E. Kalnay et al., "The NCEP/NCAR 40-year reanalysis project," *Bull. Am. Meteor. Soc.* **77**, 437–471 (1996).
19. S. Lachérade et al., "Cross-calibration over desert sites: description, methodology and operational implementation," *IEEE Trans. Geosci. Remote Sens.* **51**(3), 1098–1113 (2013).
20. X. Xiong et al., "Multiyear on-orbit calibration and performance of terra MODIS reflective solar bands," *IEEE Trans. Geosci. Remote Sens.* **45**(4), 879–889 (2007).
21. B. L. Markham et al., "Landsat-7 ETM+: 12 years on-orbit reflective-band radiometric performance," *IEEE Trans. Geosci. Remote Sens.* **50**(5), 2056–2062 (2012).
22. G. Chander et al., "Applications of spectral band adjustment factors (SBAF) for cross-calibration," *IEEE Trans. Geosci. Remote Sens.* **51**(3), 1267–1281 (2013).
23. P. K. E. Campbell et al., "EO-1 hyperion reflectance time series at calibration and validation sites: stability and sensitivity to seasonal dynamics," *IEEE J. Sel. Top. Appl. Earth Obs. Remote Sens.* **6**(2), 276–290 (2013).
24. J. McCorkel, K. Thome, and L. Ong, "Vicarious calibration of EO-1 hyperion," *IEEE J. Sel. Top. Appl. Earth Obs. Remote Sens.* **6**(2), 400–407 (2013).
25. https://earthexplorer.usgs.gov/.
26. https://ladsweb.modaps.eosdis.nasa.gov/missions-and-measurements/.
27. "MRT Swath user's manual," https://lpdaac.usgs.gov/sites/default/files/public/MRTSwath_Users_Manual_2.2_Dec2010.pdf.
28. A. Wu and Q. Zhong, "A method for determining the sensor degradation rates of NOAA AVHRR channels 1 and 2," *J. Appl. Meteorol.* **33**(1), 118–122 (1994).
29. S. A. Ackerman and R. Frey, "MODIS atmosphere L2 cloud mask product (35_L2)," NASA MODIS Adaptive Processing System, Goddard Space Flight Center (2015).
30. N. Mishra et al., "Absolute calibration of optical satellite sensors using Libya 4 pseudo invariant calibration site," *Remote Sens.* **6**(2), 1327–1346 (2014).
31. A. A. Kokahnovsky, M. Schreier, and W. VonHoyningen-Huene, "The comparison of spectral top-of-atmosphere reflectances measured by AATSR MERIS and SCIAMACHY onboard ENVISAT," *IEEE Trans. Geosci. Remote Sens.* **5**(1), 53–56 (2008).
32. D. R. Doelling et al., "Spectral reflectance corrections for satellite intercalibrations using SCIAMACHY data," *IEEE Geosci. Remote Sens. Lett.* **9**(1), 119–123 (2012).

33. B. R. Scarino et al., "A web-based tool for calculating spectral band difference adjustment factors derived from SCIAMACHY hyperspectral data," *IEEE Trans. Geosci. Remote Sens.* **54**(5), 2529–2542 (2016).
34. M. Kaewmanee, H. Vuppula, and D. Helder, "Improved temporal resolution of pseudo invariant calibration sites (PICS) through development of the PICS normalization process (PNP)," in *Proc. of CALCON* (2017).

Amit Angal received his MS degree in electrical engineering from South Dakota State University, Brookings, South Dakota, USA. Currently, he is a lead optical engineer and a supervisor with Science Systems and Applications, Inc., Lanham, Maryland, USA, where he is involved in the radiometric characterization and calibration of remote sensing instruments. He is primarily involved in the on-orbit calibration of the reflective solar bands of the Moderate-Resolution Imaging Spectroradiometer (MODIS) instruments on board the terra and aqua spacecraft. He has also supported the CLARREO Mission Preformulation activities in the reflective solar spectrum. In addition, he supports the preflight calibration of the JPSS-2 VIIRS instrument and is involved with the early on-orbit calibration and validation of the JPSS-1 VIIRS instrument. His research interests include cross-calibration between Landsat and MODIS instruments.

Xiaoxiong Xiong received his BS degree in optical engineering from Beijing Institute of Technology, Beijing, China, and his PhD in physics from the University of Maryland, College Park, Maryland, USA. Before joining the NASA Goddard Space Flight Center (GSFC), Greenbelt, Maryland, USA, he was involved in optical instrumentation, nonlinear optics, laser and atomic spectroscopy, and resonance ionization mass spectrometry at universities, industry, and the National Institute of Standards and Technology. Currently, he is an optical physicist with GSFC, where he is also serving as the Moderate Resolution Imaging Spectroradiometer (MODIS) project scientist and the technical lead for the MODIS Characterization Support Team and the VIIRS Calibration Support Team.

Dennis Helder has been involved with the characterization and calibration of spaceborne and airborne remote sensing imaging systems for over 30 years. Initial work focused on characterization and removal of radiometric artifacts of the Landsat TM and MSS sensors. More recent work has emphasized development of vicarious radiometric calibration approaches for a variety of optical remote sensing systems as well as on-orbit point spread function estimation. He has served on several NASA and USGS EROS science teams, including Landsat 7, Landsat 8, and EO-1. Currently, he is an associate dean for Engineering Research and distinguished professor of electrical engineering at South Dakota State University and is also on detail to USGS EROS as director of the EROS CalVal Center of Excellence

Morakot Kaewmanee was involved with Thailand Earth Observation Satellite (Thaichote) managing data acquisition and production system and image quality control from 2008 to 2011 (GISTDA-Geo-Informatics and Space Technology Development Agency). She came to SDSU as a visiting scientist in 2012. She has been employed as an imaging engineer I for the Image Processing Lab since 2015. She has various research interests in utilizing PICS as a calibration source, developing algorithm to improve satellite trending analysis. She received her MS degree in spatial information system in engineering, Chulalongkorn University, Thailand, and her BS degree in land information (surveying), Royal Melbourne Institute of Technology, Australia.